

DIFFender: Diffusion-Based Adversarial Defense against Patch Attacks in the Physical World

Caixin Kang¹, Yinpeng Dong², Zhengyi Wang², Shouwei Ruan¹,
Hang Su², Xingxing Wei^{1*}

¹ Institute of Artificial Intelligence, Beihang University

²Dept. of Comp. Sci. & Tech., BNRist Center, Tsinghua-Bosch Joint ML Center, Tsinghua University
 {caixinkang, shouweiruan, xxwei}@buaa.edu.cn;
 {dongyinpeng, suhangss}@tsinghua.edu.cn; wang-zy21@mails.tsinghua.edu.cn

Abstract

Adversarial attacks in the physical world, particularly patch attacks, pose significant threats to the robustness and reliability of deep learning models. Developing reliable defenses against patch attacks is crucial for real-world applications, yet current research in this area is severely lacking. In this paper, we propose DIFFender, a novel defense method that leverages the pre-trained diffusion model to perform both localization and defense against potential adversarial patch attacks. DIFFender is designed as a pipeline consisting of two main stages: patch localization and restoration. In the localization stage, we exploit the intriguing properties of a diffusion model to effectively identify the locations of adversarial patches. In the restoration stage, we employ a text-guided diffusion model to eliminate adversarial regions in the image while preserving the integrity of the visual content. Additionally, we design a few-shot prompt-tuning algorithm to facilitate simple and efficient tuning, enabling the learned representations to easily transfer to downstream tasks, which optimize two stages jointly. We conduct extensive experiments on image classification and face recognition to demonstrate that DIFFender exhibits superior robustness under strong adaptive attacks and generalizes well across various scenarios, diverse classifiers, and multiple attack methods.

1 Introduction

Deep neural networks are shown to be vulnerable to adversarial examples [25; 7], in which imperceptible perturbations are intentionally added to input examples, leading to incorrect predictions with high confidence in the model. Many adversarial attacks and defenses are devoted to studying the ℓ_p norm-bounded threat models [7; 3; 5; 17], which assume that the adversarial perturbations are restricted by the ℓ_p norm to be imperceptible. However, the classic ℓ_p perturbations require modification of every pixel of the images, which is typically not practical in the physical world. On the other hand, adversarial patch attacks [2; 13; 26; 1; 14], which usually apply perturbations to a localized region of the objects, are more physically realizable. Adversarial patch attacks pose significant threats to real-world applications, such as face recognition [22; 28], autonomous driving [12; 34].

Despite the significant efforts to defend against ℓ_p -norm perturbations in the digital world, there is less work on defending against patch attacks, which is arguably more critical to ensure the safety and reliability of real-world applications. Some existing methods [8; 19; 16; 31] try to detect and remove adversarial patches for robust recognition. However, there are still some challenges to developing an effective defense mechanism against patch attacks. First, most methods can only defend against

*Corresponding Authors.

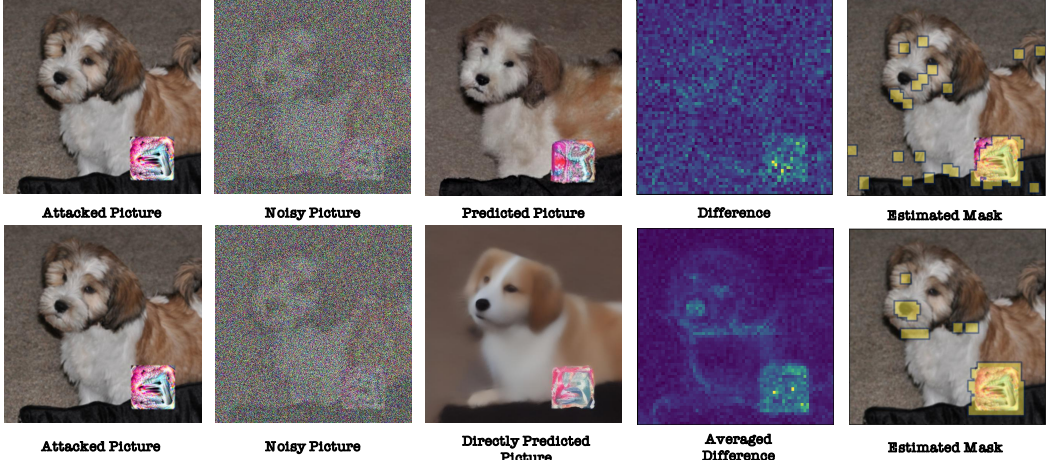


Figure 1: The intriguing property of diffusion. **Top:** The difference between diffusion predicted picture and input picture can be used to locate the patch. **Bottom:** Direct prediction of image latents using text-guided diffusion to locate patch through averaged difference(details in Sec. 4.1).

a specific attack method, which is not generalizable under diverse patch attacks considering the complex real-world scenarios. Second, some methods cause gradient obfuscation [1], which stronger adaptive attacks can further evade. Third, the existing methods cannot recover the original images with high fidelity, exhibiting substantial differences between the recovered image and the original one and leading to visual artifacts that could affect the recognition of the recovered images.

Recently, diffusion models [23; 10] have emerged as a powerful family of generative models, and have been successfully applied to improving adversarial robustness by purifying the input data [20]. By diffusing the adversarial examples with Gaussian noises and recovering the original inputs through the reverse denoising process of diffusion models, the downstream classifiers can correctly recognize the denoised images with high robustness. Our initial intuition is to explore whether diffusion purification can be applied to defend against patch attacks. However, we observe that the patch region in the adversarial image can hardly be denoised towards the clean image while the output also differs from the raw patch. But other regions outside the adversarial patch can be restored accurately, as shown in Fig. 1. This indicates that diffusion purification [20] cannot be directly used for purifying adversarial patches since they change the semantics significantly, but also suggests the potential to adopt diffusion models to detect the adversarial patch region by comparing the differences between the original adversarial example and the denoised one.

Based on the above observation, we propose **DIFFender**, a novel defense method against adversarial patch attacks based on diffusion models. DIFFender leverages the pre-trained diffusion model to perform both localization and restoration of potential adversarial patches to protect the object recognition models from patch attacks. In the localization stage, we leverage the intriguing property of the diffusion model mentioned above by subtracting the denoised image from the original adversarial image to effectively identify the locations of adversarial patches. Building upon this, we incorporate a text-guided diffusion model that utilizes visual-language pre-training to explore an open-ended visual concept space. Additionally, we design a few-shot prompt-tuning algorithm to facilitate simple and efficient tuning, enabling the learned representations to easily transfer to downstream tasks and enhancing the performance of the DIFFender. In the restoration stage, we employ a text-guided diffusion model to remove the adversarial regions from the image while preserving the underlying content. The pipeline of DIFFender is illustrated in Fig. 2.

We conduct extensive experiments on image classification and further validate our approach on face recognition. Our research findings demonstrate that DIFFender exhibits superior robustness even under strong adaptive attacks, without significantly impacting the model’s performance on clean data. Furthermore, DIFFender extends the generalization capability of pre-trained large models to various scenarios, diverse classifiers, and defense against multiple attack methods, requiring only a few-shot prompt-tuning. We demonstrate that DIFFender significantly reduces the success rate of physical patch attacks while producing more realistic restored images.

2 Related work

2.1 Adversarial attacks

The outputs of deep neural networks (DNNs) can be manipulated to produce erroneous results by introducing small perturbations to input examples. Previous attack methods, such as FGSM [7], DeepFool [18], PGD [17], and MIM [5], typically induce misclassification or detection errors by adding small perturbations to the pixels of input examples. However, while these methods can effectively generate adversarial examples in the digital world, they lack practicality in the real world.

Adversarial patch attacks, aim to deceive models by adding specific small modifications, often in the form of a pattern or sticker, to input images. These carefully designed patches can mislead the model, causing it to classify and detect the images incorrectly. These attacks can be categorized into two categories. Meaningless patch attacks include the attacks like “Adversarial Patch” by Karmon et al. [2], which generate localized and visible random perturbations, and then [13; 14]. On the other hand, meaningful patch attacks involve the use of stickers that have real-world significance. For example, Wei et al. [26] utilize stickers commonly in daily life and evaluation criteria in a black-box environment. Additionally, [28; 33] also explores meaningful patch attacks.

2.2 Adversarial defenses

With the rapid development of attacks, various defense methods have been proposed. However, most existing defenses primarily focus on global perturbations with ℓ_p norm constraints, and only a few defenses specifically address patch attacks. Some of the defense measures proposed so far include Digital Watermarking [8], Local Gradient Smoothing [19], PatchGuard [27], Feature Normalization and Clipping [31] and SentiNet [4]. For instance, the DW method utilizes saliency maps to detect adversarial regions and employs erosion and dilation operations to remove small holes. LGS suggests performing gradient smoothing on regions with high gradient amplitudes, taking into account the high-frequency noise introduced by patch attacks. FNC and PatchGuard require knowledge of the network structure and involve gradient clipping or smoothing operations on images to reduce informative class evidence. SentiNet, on the other hand, utilizes Grad-CAM to obtain masks.

However, these methods have certain limitations. They often lack generality as they heavily rely on the structure of subsequent classifiers, or they fail to effectively handle stronger adaptive attacks. In contrast, DIFFender can adapt to various scenarios and attack methods without the need for retraining. Leveraging the diffusion framework, it maintains robustness in adaptive attacks.

3 Preliminary: diffusion models

Denoising diffusion probabilistic models (DDPM) [10] is a probabilistic model that utilizes diffusion steps to transform a simple distribution into the target data distribution. This process can be seen as gradually reducing the noise while generating samples, thereby producing more realistic samples.

Since the backward process cannot be directly implemented, a neural network is trained to approximate the backward process by minimizing a denoising objective. The simplified optimization objective, without the coefficients, is

$$L_{t-1}^{\text{simple}} = \mathbb{E}_{\mathbf{x}_0, \epsilon \sim \mathcal{N}(\mathbf{0}, \mathbf{I})} \left[\|\epsilon - \epsilon_\theta(\sqrt{\alpha_t} \mathbf{x}_0 + \sqrt{1 - \alpha_t} \epsilon, t)\|^2 \right], \quad (1)$$

where \mathbf{x}_0 is the initial sample, α_t is an adjustable coefficient that controls the magnitude of noise which is a decreasing function of the timestep t , and $\bar{\alpha}_t$ is the normalized α_t , ϵ is a noise vector sampled from the distribution $\mathcal{N}(\mathbf{0}, \mathbf{I})$, ϵ_θ is the noise estimator which aims to find the noise ϵ .

Song et al. [24] proposed Denoising Diffusion Implicit Model (DDIM) to accelerate the sampling process of DDPM. DDIM and DDPM share the same training objective, but DDIM does not impose the restriction that the diffusion process must be a Markov chain. Since a smaller number of steps can be set compared to the original process, the generation process can be accelerated. The generation process can be expressed as:

$$\mathbf{x}_{\tau_{i-1}} = \sqrt{\alpha_{\tau_{i-1}}} \left(\frac{\mathbf{x}_{\tau_i} - \sqrt{1 - \alpha_{\tau_i}} \epsilon_\theta(\mathbf{x}_{\tau_i}, \tau_i)}{\sqrt{\alpha_{\tau_i}}} \right) + \sqrt{1 - \alpha_{\tau_{i-1}} - \sigma_{\tau_i}^2} \cdot \epsilon_\theta(\mathbf{x}_{\tau_i}, \tau_i) + \sigma_{\tau_i} \epsilon, \quad (2)$$

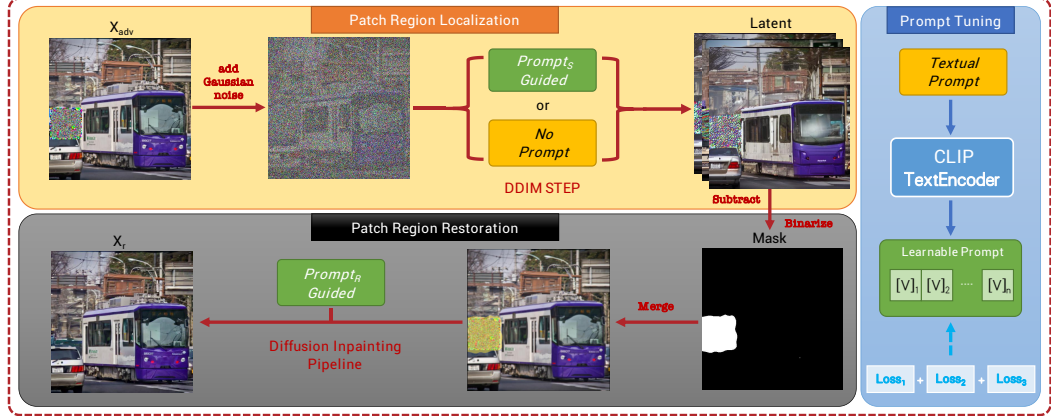


Figure 2: Pipeline of DIFFender. DIFFender leverages diffusion for the localization and restoration of adversarial attacks, and combines a prompt-tuning module to facilitate efficient tuning.

where τ_i is an index of a time step, representing different stages in the generation process, $\epsilon_\theta(\mathbf{x}_{\tau_i}, \tau_i)$ is a noise vector processed by the neural network θ and used for denoising operations in the reverse process, the variance $\sigma_{\tau_i}^2 \in \mathbb{R}$, which results in different distributions.

Then, diffpure[20] first applied diffusion models to enhance model robustness by utilizing them for adversarial purification. However, DiffPure primarily focuses on defending against global perturbations with ℓ_p -norm constraints and does not perform well against patch attacks in the physical world (analysis can be found in Section 5.2). This highlights the necessity of proposing DIFFender, which specifically addresses the challenges posed by patch attacks.

4 Methodology

In this section, we detail the proposed **DIFFender**. Fig. 2 shows the pipeline of DIFFender, which consists of three main stages: patch localization, patch restoration and prompt tuning. In the following, we introduce the overall framework of DIFFender in Sec. 4.1 and detail the improved techniques by prompt tuning in Sec. 4.2.

4.1 DIFFender

First, we introduce the problem formulation of the adversarial defense against physical patch attacks. An adversarial patch is usually applied to a restricted region of the image to be physically realizable, which can be formulated as

$$x_{adv} = (1 - M) \odot x + M \odot x_p, \quad (3)$$

where the mask M is used to indicate the adversarial regions, x_p is the adversarial image containing the patch for attack, x represents the clean example, and \odot denotes the Hadamard product. For defense, our goal is to accurately predict the location of the mask M and remove the adversarial effects from x_p .

Building upon the previous discussion, DIFFender is motivated by an intriguing observation in practical applications of diffusion models. We discover that adversarial regions in an image, which are affected by adversarial noise, are often challenging to restore to their original states using the forward and reverse processes of a diffusion model. Furthermore, the regions to be restored may vary across different attempts. However, regions outside the adversarial patches can be successfully restored easily. This observation indicates that the difference between the original and restored images can be leveraged to detect the region of the adversarial patch. Based on these insights, we propose DIFFender, a defense approach that leverages a diffusion model to locate and restore patch attacks. The pipeline of DIFFender is illustrated in Fig. 2. The entire pipeline of DIFFender is divided into three modules: Patch Region Localization, Patch Region Restoration, and Prompt Tuning.

4.1.1 Patch Localization

Given the attacked image \mathbf{x}_{adv} as input, we first add Gaussian noise to create noisy image \mathbf{x}_t , with the degree of Gaussian noise discussed in Appendix. Next, we apply the diffusion model to denoise

\mathbf{x}_t . Initially, we use a text-agnostic diffusion model to completely restore \mathbf{x}_t to a denoised image \mathbf{x}_0 . We estimate the mask region \mathbf{M}_e by taking the difference between \mathbf{x}_{adv} and the denoised image \mathbf{x}_0 . However, the diffusion model incurs a significant time cost due to the time steps T required. To address this issue, we set the time step T to 1, directly predicting the image \mathbf{x}_0 from the noisy image \mathbf{x}_t . We then average the differences between intermediate latent results l_x and l_y (latent are divided into two groups: x and y for difference) m times (with a default repetition number of m set to 3) to replace the complete diffusion process, thus reducing the prediction time. Although the directly predicted results often exhibit differences and increased blurriness compared to the original image, they are still sufficient for locating adversarial regions, as shown in Fig. 1.

$$M_e = \text{Binarize}\left(\frac{1}{m} \sum_{i=0}^m (l_x^i - l_y^i)\right) \quad (4)$$

During diffusion denoising, we can employ text-agnostic diffusion or use prompt-guided diffusion for prediction. The prompt used can be a manually crafted text prompt such as 'adversarial' or a learnable text vector, which improves the performance of region localization. This introduces the prompt-tuning module, where we convert the input *text* into a learnable word vector *prompt* of length n . Further details on the prompt-tuning module will be discussed in Sec. 4.2

4.1.2 Patch Restoration

The restoration step is to eliminate the adversarial properties of adversarial regions, also consider preserving the overall coherence and quality of the image. We binarize the latent difference obtained from the previous step to estimate the \mathbf{M}_e region. Then, we combine the mask and \mathbf{x}_{adv} as inputs to the text-guided DDIM. For the mask processing, we follow the approach of the Stable-Diffusion-Inpainting [21] pipeline, where a UNet is used with an additional five input channels to incorporate the mask \mathbf{M}_e estimated by the DIFFender Localization. Similarly, the $prompt_R$ can be optimized using the prompt-tuning module to obtain the optimal text vector representation, which guides the diffusion process for denoising. Finally, we obtain the restored clean image x_r .

4.2 Prompt Tuning

Following the aforementioned pipeline, DIFFender is capable of efficiently performing patch localization. While in most cases it accurately segments the adversarial regions within the image, there are certain instances where the segmented mask exhibits minor discrepancies. Visual language pretraining enables the exploration of an expansive semantic space by leveraging a high-capacity text encoder. In order to facilitate the transferability of the learned representations to downstream tasks, we introduce the concept of prompt tuning.

Learnable prompts. Firstly, we replace the textual vocabulary with learnable continuous vectors. Specifically, the $text_s$ provided to DIFFender segmentation module and the $test_r$ used to guide the restoration process in DIFFender are transformed into prompt vectors in the following format:

$$prompt_S = [V_S]_1 [V_S]_2 \dots [V_S]_n; \quad prompt_R = [V_R]_1 [V_R]_2 \dots [V_R]_n, \quad (5)$$

where each $[V_S]_i$ or $[V_R]_i$ ($i \in \{1, \dots, n\}$) is a vector of the same dimensionality as word embeddings. Here, we utilize the CLIP model, which has word embeddings of length 512. n is a hyperparameter that specifies the number of context tokens. We set this value to 16 by default.

The text content used to initialize $prompt_S$ and $prompt_R$ can be manually provided, as mentioned earlier, such as 'adversarial' or 'clean'. Alternatively, it can be randomly initialized generated text. By forwarding $prompt_S$ and $prompt_R$ to the text encoder $gCLIP(\cdot)$ of the CLIP model, we obtain the clip text embedding vectors E_c that correspond to the visual concepts described by the text.

$$E_c = gCLIP(prompt) \quad (6)$$

Tuning process. After obtaining the learnable text vectors, we designed three distinct loss functions to ensure the effectiveness of prompt-tuning, which jointly optimize the prompt vector to better capture the characteristics of the adversarial regions and improve the defense performance.

Firstly, for the diffusion segmentation component, we employ the cross-entropy loss to compute the $loss_1$ value by comparing the estimated mask \mathbf{M}_e with the ground truth mask \mathbf{M} , to accurately

identify the adversarial regions through diffusion segmentation.

$$L_{CE}(x) = - \sum_{i=1}^n \mathbf{M}(x_i) \log(\mathbf{M}_e(x_i)). \quad (7)$$

Next, in the DIFFender restoration module, our objective is to reconstruct and restore the mask regions while eliminating the adversarial effects on the image. To ensure effective repair, we employ the L1 loss to calculate the $loss_2$ value between the reconstructed image x_r and the clean image x_c as

$$L_1 = |x_r - x_c|. \quad (8)$$

Lastly, to verify that the adversarial properties have been eliminated. We carry $loss_3$ which draws inspiration from the discussion on image adversarial properties [15] and leverage the concept of “Learned Perceptual Image Patch Similarity” mentioned in [32]. To compute $loss_3$, the outputs of each layer are activated and compute the L2 distance by performing element-wise multiplication with weights in w layers. Finally, the distances are average to obtain the value of $loss_3$.

$$d(x_r, x_c) = \sum_l \frac{1}{H_l W_l} \sum_{h,w} \|w_l \odot (\hat{y}_{rhw}^l - \hat{y}_{chw}^l)\|_2^2, \quad (9)$$

where l denotes a certain layer in the network, $\hat{y}_r^l, \hat{y}_c^l \in \mathcal{R}^{H_l \times W_l \times C_l}$ are the unit-normalize results in the channel dimension, and vector $w^l \in \mathcal{R}^{C_l}$ is used for scaling activation channels.

By summing up the aforementioned three losses and allowing gradients to propagate through the entire pipeline of DIFFender and the text encoder gCLIP, we can optimize the $promptS$ and $promptR$ utilizing the rich knowledge encoded in the parameters. The design of continuous representations also enables thorough exploration in the embedding space.

$$Loss_{DIFF} = loss_1 + loss_2 + loss_3 \quad (10)$$

Few-shot. During prompt-tuning, we utilize a minimal number of images for few-shot training. Specifically, DIFFender is trained on a limited set of attacked images from a single scenario and targeted at a specific attack method, but can still learn optimal prompts that generalize well to other scenarios and attacks, which makes the tuning straightforward and results in a short time requirement.

5 Experiments

5.1 Evaluation on ImageNet

Experimental settings. For attacks, we employ AdvP [2] and LaVAN [13], which randomly select patch positions and generate perturbations using different loss functions. We also employ GDPA [14] which optimizes the patch’s position and content to execute attacks. We set the patch size to 50 for AdvP, 30 for LaVAN, and 30 for GDPA to introduce attacks of different sizes and set the number of iterations for the attacks to 100. To adaptively attack the baseline defense based on preprocessing, we approximate gradients using the BPDA [1] method. For adapting the attack on DIFFender, we use Straight-Through Estimator (STE) [30] during backpropagation through thresholding operations. Additionally, due to the randomness introduced by the diffusion and denoising processes, we apply an adaptive attack using the Expectation over Transformation (EOT) + BPDA attack [1]. We compared DIFFender with five defense methods: Image smoothing-based defenses, including JPEG [6] and Spatial Smoothing [29]; Image completion-based defenses, such as DW [8], LGS [19]; Feature-level suppression defense FNC [31]. Default parameters for defenses are obtained from their papers. We then selected two advanced classifiers trained on ImageNet as the threat models: CNN-based Inception-V3 and Transformer-based Swin-S. The implementation details are provided in Appendix.

Evaluation metrics. We evaluated the performance of defense methods under standard accuracy and robust accuracy. Due to the high computational cost of applying our method with adaptive attacks, unless otherwise specified, we assessed the robustness accuracy of our method and previous methods on a fixed subset of 256 sampled images from the test set. To facilitate the observation of changes, we ensured that the selected subset consisted of images correctly classified by all classifiers.

Table 1: The accuracy (%) under different attack and defense methods. "NP", "HP", and "PT" represent "No prompt", "Manual prompt" and "Prompt tuning" versions of DIFFender, respectively.

Defense	Inception-V3				Swin-S			
	Clean	AdvP	LaVAN	GDPA	Clean	AdvP	LaVAN	GDPA
Undefended	100.0	0.0	8.3	64.8	100.0	1.5	3.4	78.1
JPEG [6]	48.7	0.5	15.4	64.8	85.0	0.6	5.8	77.0
SS [29]	72.8	1.0	14.9	57.8	86.4	2.4	5.4	68.8
DW [8]	87.2	1.0	9.2	62.5	98.1	0.0	4.9	77.3
LGS [19]	87.7	55.4	50.3	67.2	89.8	65.6	59.7	82.0
FNC [31]	91.0	61.5	64.9	66.4	91.7	6.4	7.4	77.0
DIFFender (NP)	91.3	60.7	32.8	71.1	93.2	52.2	32.0	79.3
DIFFender (MP)	90.8	67.1	48.7	70.3	92.7	80.0	53.4	77.0
DIFFender (PT)	88.4	81.5	70.0	74.2	90.2	89.8	83.5	79.7

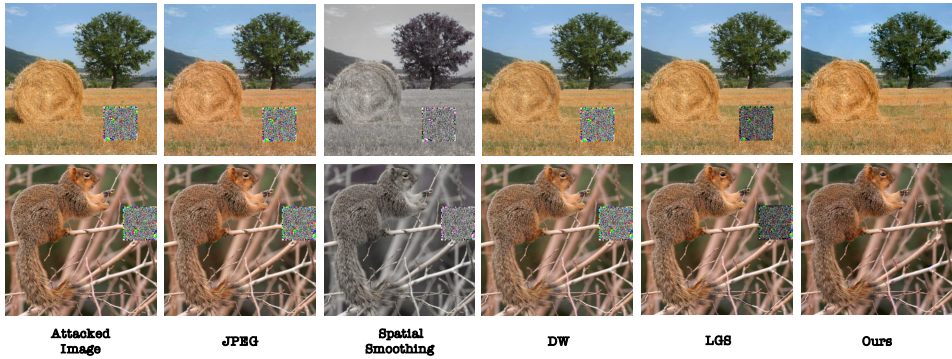


Figure 3: Visualization results with examples from ImageNet adaptively attacked by AdvP. Compared with the other four defense methods, the restored results of DIFFender no longer show any traces of the patch, and the restored details are remarkable.

Experimental results. Tab. 1 presents the experimental results, where the highest accuracy is highlighted in bold. We compare DIFFender with 5 baselines. For DIFFender with manual prompts, we set $prompt_S$ ="adversarial" and $prompt_R$ ="clean", for prompt-guided DIFFender, we randomly initialize $prompt_S$ and $prompt_R$. Based on these results, we draw the following conclusions.

(1) Compared to previous methods, DIFFender outperforms in defense effectiveness. Under strong adaptive attacks utilizing gradients, such as the AdvP and LaVAN, DIFFender exhibits superior defense performance. This can be attributed to the fact that DIFFender is built upon the diffusion framework. Intuitively, the diffusion model can effectively remove adversarial areas while ensuring a high-quality and diverse generation that closely follows the underlying distribution of clean data. Additionally, the inherent stochasticity in the diffusion model allows for robust stochastic defense mechanisms [9]. These characteristics make it a well-suited "defender" for adversarial attacks.

(2) Traditional image processing defense methods, such as JPEG, SS, and DW, experience a significant decrease in robust accuracy under strong adaptive attacks. This can be attributed to the algorithms' gradients can be easily obtained, making them vulnerable to adaptive attacks. More recent methods, such as LGS and FNC, consider the robustness against adaptive attacks. For instance, FNC achieves robust accuracy second only to DIFFender on Inception-v3. However, their defense effectiveness diminishes when applied to the Swin-s method. This is because the feature norm clipping layer proposed is specifically designed for handling CNN feature maps, while DIFFender exhibits excellent generalization capabilities that can extend to different classifiers and architectures.

(3) In the experiments, DIFFender undergoes 8-shot prompt-tuning specifically for the AdvP method. However, it still maintains good performance when facing other attack methods. This demonstrates the generalization capability of DIFFender to handle unseen attack methods.

(4) The prompt-tuned DIFFender demonstrates a significant improvement in robust accuracy compared to the other two versions of DIFFender. Even with exposure to only a few attacked images, this enhancement highlights the effectiveness of few-shot prompt tuning.

Visualization. Fig. 3 presents the final defense results of the different defense methods against patch attacks in the experiment. Since FNC suppresses the feature maps during the inference stage, it is not shown in the Fig. 3. Other methods such as JPEG and DW only exhibit minor changes in the reconstructed images and fail to defend against adaptive patch attacks. The images after spatial Smoothing defense show color distortion and are still vulnerable to adaptive patch attacks. In the case of the LGS method, the patch area is visibly suppressed, which improves the robustness accuracy to some extent, but the patch area is not completely eliminated. On the other hand, the restored images after DIFFender defense no longer shows any traces of the patch, and the restored details are remarkable (e.g., the recovery of tree branches in the second column of images). The high robustness accuracy values in Tab. 1 also indicate the removal of adversarial elements from the images.

5.2 Additional results and ablation studies

Cross-model transferability. Specifically, we conducted 8-shot prompt-tuning using the AdvP method on both Inception-v3 and Swin-S models. We then tested the transferability of learned prompts on CNN-based ResNet50 and transformer-based ViT-B-16 models. The results are presented in Tab. 2. It can be observed that prompt-tuning results, exhibit high robust accuracy when applied to new classifiers. This indicates that prompt-tuning indeed leads to improved prompt representations, and the tuned prompts demonstrate good generalization capabilities.

Compared with Diffpure. When defending against global perturbations with ℓ_p -norm constraints, diffpure achieves excellent results compared to other methods. However, it performs poorly when facing patch attacks in the physical world. Specifically, in Tab. 3, when tested against strong adaptive attacks such as AdvP and LaVAN, the inceptionv3 model purified by diffpure only maintains robust accuracy rates of 10.4% and 15.3%, respectively. The reason for this performance difference lies in the fact that patch attacks in the physical world often introduce more severe perturbations in local regions. The diffpure method, which is designed to address global perturbations, is unable to fully purify the adversarial nature of patch attacks. This highlights the necessity of proposing DIFFender, which specifically addresses the challenges posed by patch attacks.

Loss ablation performance of DIFFender. To evaluate the effectiveness of different losses, we trained several individual models. Loss1, which supervises mask segmentation, is essential and cannot be removed. We conducted separate training experiments by removing either loss3 or loss2, and the results are presented in Tab. 4. Removing loss2 had a significant impact on the robust accuracy, although it led to an improvement in clean accuracy. On the other hand, removing loss3 had a minimal effect on the AdvP method itself, but it compromised the generalization of the tuning results and resulted in a decrease in clean accuracy.

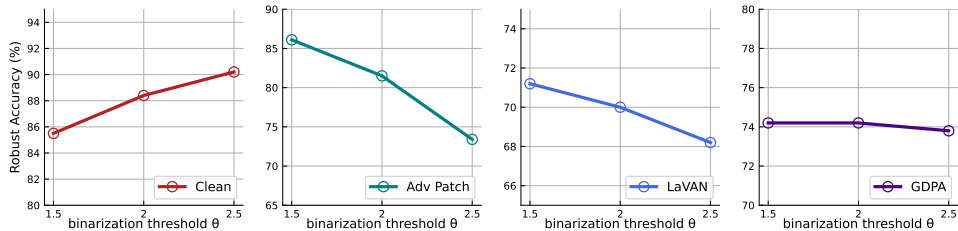


Figure 4: DIFFender performance of different binarization threshold θ on ImageNet dataset. In experiments, we set $\theta = 2.0$ to showcase the final results.

The effects of θ . The process of binarizing the latent differences to obtain a mask in the M_e estimation is a crucial step in DIFFender. As shown in Fig. 4. We compare the cases of $\theta = 1.5$ and $\theta = 2.5$. When $\theta = 1.5$, DIFFender achieves the best robust accuracy, reaching 86.1% against

Table 2: DIFFender transferability performance on ResNet50 and ViT-B-16.

Defense	ResNet-50				ViT-base			
	Clean	AdvP	LaVAN	GDPA	Clean	AdvP	LaVAN	GDPA
Undefended	100.0	0.0	14.9	73.8	100.0	1.1	1.8	76.2
DIFFender(PT)	77.0	72.1	55.6	76.2	90.3	88.2	84.6	78.9

Table 3: DIFFender performance compared with diffpure.

Defense	Inception-V3			
	Clean	AdvP	LaVAN	GDPA
Diffpure	65.1	10.4	15.3	67.6
DIFFender(PT)	88.4	81.5	70.0	74.2

AdvP attacks. However, the clean accuracy decreases slightly to 85.5%. On the other hand, when $\theta = 2.5$, the clean accuracy improves, but the robust accuracy decreases. We can observe that there is a tradeoff between clean and robust accuracy.

5.3 Extension in Face Recognition.

Experimental settings. Facial expressions in human faces introduce a rich diversity, together with external factors such as lighting conditions and viewing angles, making face recognition a challenging task in the recognition. In order to investigate this complex scenario, we conducted experiments on the LFW dataset[11], which is widely used in face recognition research. We employed two adversarial patch attack methods specifically designed for faces: RHDE[26], which utilizes realistic stickers and searches for their optimal positions to launch adversarial attacks, and GDPA [14] mentioned above.

Table 5: ACC% under different attacks and defenses on LFW.

Defense	FaceNet		
	Clean	GDPA	RHDE
Undefended	100.0	56.3	42.9
JPEG [6]	44.1	16.8	17.9
SS [29]	19.9	8.2	3.6
DW [8]	37.1	15.2	7.1
LGS [19]	60.9	71.9	53.6
FNC [31]	100.0	39.8	39.3
DIFFender (NP)	100.0	79.3	57.1
DIFFender (MP)	100.0	77.0	57.1
DIFFender (PT)	100.0	81.0	60.7

Experimental results. The results on the LFW dataset are presented in Tab. 5. The DIFFender method achieved the highest robust accuracy under both the GDPA and RHDE attack methods while ensuring that the clean accuracy did not decrease. It is worth noting that the prompt used in DIFFender for this experiment was not re-tuned specifically for facial recognition. This further demonstrates the generalizability of DIFFender across different scenarios and against different attack methods. In contrast, traditional image preprocessing methods such as JPEG, SS, and the recent FNC method obtained lower robust accuracies, even below the clean accuracy. This is because in the specific context of facial recognition, the classifier focuses more on crucial local features, and preprocessing the entire image can disrupt these important features. FNC suppresses the generation of large norm deep feature vectors in CNN classifiers, which also disrupts the facial features. These findings highlight the effectiveness of the DIFFender method in maintaining high robust accuracy while preserving important local facial features.

Visualization. Fig. 5 illustrates the defense results of DIFFender against face attacks. It can be observed that DIFFender accurately identifies the location of the patch and achieves excellent restoration. Additionally, it is noteworthy that the GDPA and RHDE attacks employ patches of different sizes and shapes compared to the above experiments. Demonstrating DIFFender’s ability to generalize to unseen patch shapes. This further emphasizes the robustness and versatility of the DIFFender method in handling diverse and previously unseen adversarial patch configurations.

6 Discussion and Conclusion

We propose **DIFFender**, a novel defense method that leverages the pre-trained diffusion model to perform both localization and restoration of patch attacks in the physical world. Additionally, we design a few-shot prompt-tuning algorithm to facilitate simple and efficient tuning. To show the robust

Table 4: Loss ablation performance of DIFFender.

Inception-V3			
loss1	loss2	loss3	Clean
✓	✓		86.1
✓		✓	90.8
✓	✓	✓	88.4
			79.2
			62.6
			73.0
			73.8
			70.0
			74.2



Figure 5: Visualization results with examples from LFW attacked by RHDE.

performance of our method, we conduct experiments on image classification and further validate our approach on face recognition. Our research findings demonstrate that DIFFender exhibits superior robustness even under strong adaptive attacks and extends the generalization capability of pre-trained large models to various scenarios, diverse classifiers, and multiple attack methods, requiring only a few-shot prompt-tuning. We demonstrate that DIFFender significantly reduces the success rate of physical patch attacks while producing realistic restored images.

Limitations: As an initial attempt of diffusion for patch defense, this work has several limitations. First, although we have designed acceleration techniques, the evaluation is conducted on a subset of 256 sampled images from the test set due to time constraints. This may introduce bias, as elaborated in the appendix. Secondly, while our method does not require training, it incurs a higher computational cost during inference. We will address these limitations in the following work.

References

- [1] Anish Athalye, Nicholas Carlini, and David Wagner. Obfuscated gradients give a false sense of security: Circumventing defenses to adversarial examples. In *International conference on machine learning*, pages 274–283. PMLR, 2018.
- [2] Tom B Brown, Dandelion Mané, Aurko Roy, Martín Abadi, and Justin Gilmer. Adversarial patch. *arXiv preprint arXiv:1712.09665*, 2017.
- [3] Nicholas Carlini and David Wagner. Towards evaluating the robustness of neural networks. In *IEEE Symposium on Security and Privacy*, 2017.
- [4] Edward Chou, Florian Tramer, and Giancarlo Pellegrino. Sentinel: Detecting localized universal attacks against deep learning systems. In *2020 IEEE Security and Privacy Workshops (SPW)*, pages 48–54. IEEE, 2020.
- [5] Yinpeng Dong, Fangzhou Liao, Tianyu Pang, Hang Su, Jun Zhu, Xiaolin Hu, and Jianguo Li. Boosting adversarial attacks with momentum. In *Proceedings of the IEEE conference on computer vision and pattern recognition*, pages 9185–9193, 2018.
- [6] Gintare Karolina Dziugaite, Zoubin Ghahramani, and Daniel M Roy. A study of the effect of jpg compression on adversarial images. *arXiv preprint arXiv:1608.00853*, 2016.
- [7] Ian J Goodfellow, Jonathon Shlens, and Christian Szegedy. Explaining and harnessing adversarial examples. *arXiv preprint arXiv:1412.6572*, 2014.
- [8] Jamie Hayes. On visible adversarial perturbations & digital watermarking. In *Proceedings of the IEEE Conference on Computer Vision and Pattern Recognition Workshops*, pages 1597–1604, 2018.
- [9] Zhezhi He, Adnan Siraj Rakin, and Deliang Fan. Parametric noise injection: Trainable randomness to improve deep neural network robustness against adversarial attack. In *Proceedings of the IEEE/CVF Conference on Computer Vision and Pattern Recognition*, pages 588–597, 2019.
- [10] Jonathan Ho, Ajay Jain, and Pieter Abbeel. Denoising diffusion probabilistic models. *Advances in Neural Information Processing Systems*, 33:6840–6851, 2020.
- [11] Gary B Huang, Marwan Mattar, Tamara Berg, and Eric Learned-Miller. Labeled faces in the wild: A database for studying face recognition in unconstrained environments. In *Workshop on faces in 'Real-Life' Images: detection, alignment, and recognition*, 2008.
- [12] Pengfei Jing, Qiyi Tang, Yuefeng Du, Lei Xue, Xiapu Luo, Ting Wang, Sen Nie, and Shi Wu. Too good to be safe: Tricking lane detection in autonomous driving with crafted perturbations. In *Proceedings of USENIX Security Symposium*, 2021.
- [13] Danny Karmon, Daniel Zoran, and Yoav Goldberg. Lavan: Localized and visible adversarial noise. In *International Conference on Machine Learning*, pages 2507–2515. PMLR, 2018.
- [14] Xiang Li and Shihao Ji. Generative dynamic patch attack. *arXiv preprint arXiv:2111.04266*, 2021.

[15] Fangzhou Liao, Ming Liang, Yinpeng Dong, Tianyu Pang, Xiaolin Hu, and Jun Zhu. Defense against adversarial attacks using high-level representation guided denoiser. In *Proceedings of the IEEE conference on computer vision and pattern recognition*, pages 1778–1787, 2018.

[16] Jiang Liu, Alexander Levine, Chun Pong Lau, Rama Chellappa, and Soheil Feizi. Segment and complete: Defending object detectors against adversarial patch attacks with robust patch detection. In *Proceedings of the IEEE/CVF Conference on Computer Vision and Pattern Recognition*, pages 14973–14982, 2022.

[17] Aleksander Madry, Aleksandar Makelov, Ludwig Schmidt, Dimitris Tsipras, and Adrian Vladu. Towards deep learning models resistant to adversarial attacks. *arXiv preprint arXiv:1706.06083*, 2017.

[18] Seyed-Mohsen Moosavi-Dezfooli, Alhussein Fawzi, and Pascal Frossard. Deepfool: a simple and accurate method to fool deep neural networks. In *Proceedings of the IEEE conference on computer vision and pattern recognition*, pages 2574–2582, 2016.

[19] Muzammal Naseer, Salman Khan, and Fatih Porikli. Local gradients smoothing: Defense against localized adversarial attacks. In *2019 IEEE Winter Conference on Applications of Computer Vision (WACV)*, pages 1300–1307. IEEE, 2019.

[20] Weili Nie, Brandon Guo, Yujia Huang, Chaowei Xiao, Arash Vahdat, and Anima Anandkumar. Diffusion models for adversarial purification. *arXiv preprint arXiv:2205.07460*, 2022.

[21] Robin Rombach, Andreas Blattmann, Dominik Lorenz, Patrick Esser, and Björn Ommer. High-resolution image synthesis with latent diffusion models. In *Proceedings of the IEEE/CVF Conference on Computer Vision and Pattern Recognition (CVPR)*, pages 10684–10695, June 2022.

[22] Mahmood Sharif, Sruti Bhagavatula, Lujo Bauer, and Michael K. Reiter. Accessorize to a crime: Real and stealthy attacks on state-of-the-art face recognition. In *ACM SigSAC Conference on Computer and Communications Security*, pages 1528–1540, 2016.

[23] Jascha Sohl-Dickstein, Eric Weiss, Niru Maheswaranathan, and Surya Ganguli. Deep unsupervised learning using nonequilibrium thermodynamics. In *International Conference on Machine Learning*, pages 2256–2265, 2015.

[24] Jiaming Song, Chenlin Meng, and Stefano Ermon. Denoising diffusion implicit models. *arXiv preprint arXiv:2010.02502*, 2020.

[25] Christian Szegedy, Wojciech Zaremba, Ilya Sutskever, Joan Bruna, Dumitru Erhan, Ian Goodfellow, and Rob Fergus. Intriguing properties of neural networks. *arXiv preprint arXiv:1312.6199*, 2013.

[26] Xingxing Wei, Ying Guo, and Jie Yu. Adversarial sticker: A stealthy attack method in the physical world. *IEEE Transactions on Pattern Analysis and Machine Intelligence*, 2022.

[27] Chong Xiang, Arjun Nitin Bhagoji, Vikash Sehwag, and Prateek Mittal. Patchguard: A provably robust defense against adversarial patches via small receptive fields and masking. In *USENIX Security Symposium*, pages 2237–2254, 2021.

[28] Zihao Xiao, Xianfeng Gao, Chilin Fu, Yinpeng Dong, Wei Gao, Xiaolu Zhang, Jun Zhou, and Jun Zhu. Improving transferability of adversarial patches on face recognition with generative models. In *Proceedings of the IEEE/CVF Conference on Computer Vision and Pattern Recognition*, pages 11845–11854, 2021.

[29] Weilin Xu, David Evans, and Yanjun Qi. Feature squeezing: Detecting adversarial examples in deep neural networks. *arXiv preprint arXiv:1704.01155*, 2017.

[30] Penghang Yin, Jiancheng Lyu, Shuai Zhang, Stanley Osher, Yingyong Qi, and Jack Xin. Understanding straight-through estimator in training activation quantized neural nets. *arXiv preprint arXiv:1903.05662*, 2019.

- [31] Cheng Yu, Jiansheng Chen, Youze Xue, Yuyang Liu, Weitao Wan, Jiayu Bao, and Huimin Ma. Defending against universal adversarial patches by clipping feature norms. In *Proceedings of the IEEE/CVF International Conference on Computer Vision*, pages 16434–16442, 2021.
- [32] Richard Zhang, Phillip Isola, Alexei A Efros, Eli Shechtman, and Oliver Wang. The unreasonable effectiveness of deep features as a perceptual metric. In *Proceedings of the IEEE conference on computer vision and pattern recognition*, pages 586–595, 2018.
- [33] Yiqi Zhong, Xianming Liu, Deming Zhai, Junjun Jiang, and Xiangyang Ji. Shadows can be dangerous: Stealthy and effective physical-world adversarial attack by natural phenomenon. In *Proceedings of the IEEE/CVF Conference on Computer Vision and Pattern Recognition*, pages 15345–15354, 2022.
- [34] Zijian Zhu, Yichi Zhang, Hai Chen, Yinpeng Dong, Shu Zhao, Wenbo Ding, Jiachen Zhong, and Shibao Zheng. Understanding the robustness of 3d object detection with bird’s-eye-view representations in autonomous driving. *arXiv preprint arXiv:2303.17297*, 2023.